Comparison of symmetrical hemodialysis catheters using computational fluid dynamics

Comparison of Symmetric Hemodialysis Catheters Using Computational Fluid Dynamics

Timothy W.I. Clark, MD, Giuseppe Isu, MS, Diego Gallo, PhD, Pascal Verdonck, PhD, and Umberto Morbiducci, PhD

ABSTRACT

Purpose: Symmetric-tip dialysis catheters have become alternative devices because of low access recirculation and ease of tip positioning. Flow characteristics of three symmetric catheters were compared based on computational fluid dynamics (CFD) as they relate to catheter function.

Materials And Methods: In Palindrome, GlidePath, and VectorFlow catheters, a computational fluid dynamics–based approach was used to assess (i) regions of flow separation, which are prone to thrombus development; (ii) shear-induced platelet activation potency; (iii) recirculation; and (iv) venous outflow deflection. A steady-state, laminar flow model simulated catheter tip position within the superior vena cava. Catheter performance was investigated at high hemodialysis flow rate (400 mL/min). Blood was assumed as a Newtonian fluid.

Results: Wide regions of flow separation downstream of the Palindrome side slot and close to the distal tip were observed in forward and reversed line configurations. Geometric asymmetry of the distal guide wire aperture of the GlidePath catheter produced the highest levels of inverted velocity flow when run in reversed configuration. The lowest mean shear-induced platelet activation was exhibited by GlidePath and VectorFlow catheters; the Palindrome catheter exhibited 152% higher overall platelet activation potency. All catheters were associated with a recirculation close to zero; the helically contoured lumens of the VectorFlow catheter produced the greatest amount of deflection of venous flow away from the arterial lumen.

Conclusions: The VectorFlow catheter produced less shear-induced platelet activation than the Palindrome catheter and less flow separation than the Palindrome and GlidePath catheters irrespective of line configuration. These findings have potential implications for differences in thrombogenic risk during clinical performance of these catheters.

ABBREVIATIONS

CFD = computational fluid dynamics, PAS = platelet activation state, SVC = superior vena cava, 3D = three-dimensional

More than 400,000 Americans receive renal replacement therapy through hemodialysis. Despite native fistula placement being the preferred form of permanent access, catheters remain the initial access for the majority of patients in the United States, and they serve as a "bridge" to new access creation in patients with failed arteriovenous access (1).

Catheter thrombosis and infection remain causes of vascular access–related morbidity (2). Catheter performance during dialysis is also a challenge, as the use of catheters with higher recirculation and/or reduced clearance will result in inadequate dialysis sessions (3). Inadequate dialysis has been shown to be an independent predictor of increased hospitalizations, hospital days, and Medicare inpatient expenditures among patients receiving hemodialysis (4).

Differences in catheter tip design can produce significant differences in flow characteristics during the high-flow conditions required during dialysis, and in turn can have important implications for catheter thrombogenicity, recirculation, and other critical parameters of catheter performance (5). Symmetric-tip catheters have become alternatives to conventional step-tip and split-tip catheters,

From the Section of Interventional Radiology, Department of Radiology (T.W.I.C.), University of Pennsylvania School of Medicine, 39th and Market Sts., Philadelphia, PA 19104; Department of Mechanical and Aerospace Engineering (G.I., D.G., U.M.), Politecnico di Torino, Turin, Italy; and Institute Biomedical Technology (P.V.), Ghent University, Ghent, Belgium. Received August 14, 2014; final revision received October 27, 2014; accepted November 1, 2014. **Address correspondence to** T.W.I.C.; E-mail: timothy.clark@uphs.upenn.edu

T.W.I.C. has a royalty agreement with Teleflex (Wayne, Pennsylvania). None of the other authors have identified a conflict of interest.

Appendix E1, Figure E1, and Videos E1-E6 are available online at *www.jvir.org*.

J Vasc Interv Radiol 2015; 26:252–259

http://dx.doi.org/10.1016/j.jvir.2014.11.004

in part because of the ability to reverse lines during dialysis without an increase in recirculation (6). These differences were assessed among three commercially available symmetrical tip catheters with the use of computational fluid dynamics (CFD), as widely applied to study the hemodynamic performance of catheters (7–9).

MATERIALS AND METHODS

Computational Fluid Dynamics

CFD simulations were designed to investigate and compare local hemodynamics in three commercially available symmetric-tip dialysis catheters: Palindrome (Covidien, Dublin, Ireland), GlidePath (Bard Access Systems, Salt Lake City, Utah), and VectorFlow (Teleflex, Wayne, Pennsylvania). High-resolution computer-aided design models of each catheter (**Fig 1**) were created as follows: the Palindrome catheter was measured with a touch probe coordinate machine, and the resultant measurements were used to generate a high-resolution three-dimensional (3D) model in SolidWorks (Dassault Systems, Vélizy-Villacoublay, France). For the GlidePath catheter, internal and external surfaces were scanned within a high-resolution industrial computed tomography system (GKS Services, Minneapolis, Minnesota), and the resulting 3D dataset was then rendered into SolidWorks. Both techniques ensured high accuracy in the reconstruction of every geometric characteristic of the catheter models. The VectorFlow catheter was rendered by using design-control SolidWorks files. The 3D models were coaxially placed inside a cylindrical conduit (as detailed later) ideally resembling the SVC and processed to build discrete grids (in which the governing equations of fluid motion have to be numerically solved) by using the general-purpose solid modeler ICEM (ANSYS, Canonsburg, Pennsylvania). The computational grid consisted of more than 8 million discrete tetrahedral/hexahedral cells (0.2-mm average edge size).

Model Assumptions

A previously validated CFD model (9) was used to simulate catheter tip position within the SVC, as it is currently not feasible to simulate hemodialysis catheters within a robust right atrial model because of the complexity of assumptions regarding atrial anatomy, proportion of flow from the inferior vena cava, and tricuspid valvular function. The SVC flow conditions were realistically assumed as 3 L/min within an 18-mm-diameter, 480-mm-long conduit with standard assumptions of adult human blood (uncompressible Newtonian fluid model [10] with viscosity μ 3.5 mPa · s and density ρ 1,060 kg/m^3). Catheter performance was evaluated at a 400 mL/min flow rate, in accordance with optimal clinical practice, with the catheters run in forward and reversed line configurations. A detailed description of the methodology applied to prescribe the conditions at boundaries is available in **Appendix E1** (available online at *www.jvir.org*).

CFD Simulations and Postprocessing

For all models, flow fields were computed by solving the 3D, steady-state (assumption based on the low pulsatility characterizing venous flow) governing equations of fluid motion in discrete form by using a finite volume-based commercial code (Fluent; ANSYS). Each catheter was initially studied by using classical fluid-dynamic theoretical analysis, which verified the soundness of the assumption of flow laminarity. Sensitivity analysis was carried out to assure grid-independence of the solution. Each catheter was run in forward and reversed directions to simulate clinical practice. A detailed description of the computational settings is provided in **Appendix E1**.

Analysis of Thrombogenic Flow Patterns Inside Catheters

The thrombogenic potency of the geometric features of the catheters was evaluated in terms of position and

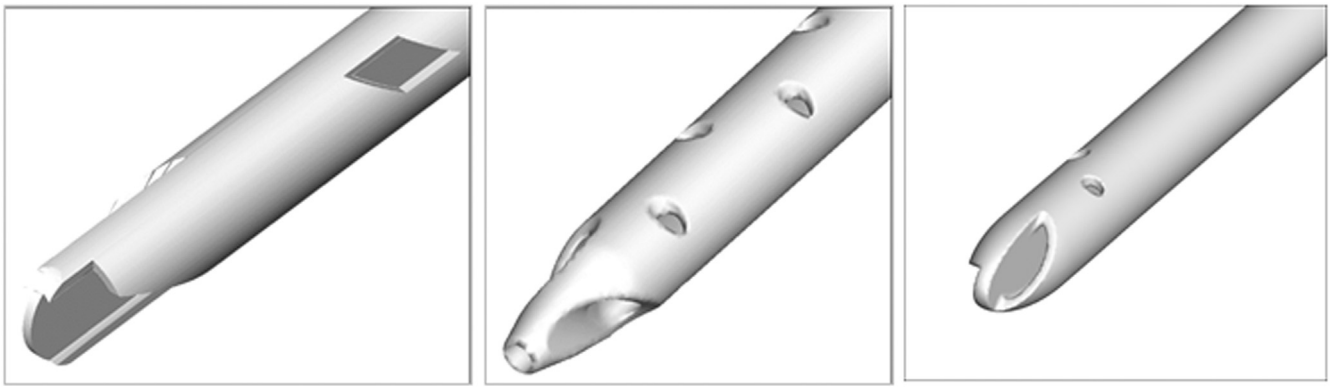

Figure 1. Three-dimensional computer-aided design models of the Palindrome **(a)**, GlidePath **(b)**, and VectorFlow **(c)** catheters before tetrahedral/hexahedral meshing for analysis using CFD. The Palindrome catheter is completely symmetric. The GlidePath catheter is not perfectly symmetric; it has a guide wire aperture at the distal tip as part of the venous lumen, as well as offset side holes. The VectorFlow catheter has complete symmetry of its distal tip but offsetting of its side holes.

dimension of the flow-separation regions (ie, the boundary layers of flow that separate from the wall of the catheter to form a recirculation vortex behind the separation point where shear stress vanishes to become zero) generated within the lumens of the catheters as a result of shape, size, number and position of the distal tip and side holes. From a hemodynamic standpoint, flow separation occurs in regions of disturbed flow, where it can promote thrombus formation and development. Flow separation regions of each catheter were visually rendered by color-encoding the 3D isosurfaces of blood velocity components with flow in the direction opposite to the main direction of the flow.

To further characterize the thrombogenic potency of flow patterns, the percentage volume of blood within each catheter model experiencing flow inversion (ie, flow in the opposite direction to the main direction of flow) was also calculated. To do this, the arterial blood lumen inside a catheter segment of length extending from the tip to a 5.0-cm distance from the more distal side hole was considered.

Analysis of Shear-Induced Platelet Activation

As in previous studies of blood-recirculating devices (11), to gain better understanding of the mechanisms that lead to flow-induced thrombogenic complications, the relationship between catheter-induced hemodynamics and platelet activation was quantified. A previously validated Lagrangian-based mathematical model was used (12), accounting for cumulative dynamic shear conditions experienced by platelets, and is expressed as the platelet activation state (PAS) (13). PAS quantifies the more global thrombogenic aspect of platelet prothrombinase activity, ie, its contribution to thrombin generation; PAS values are expressed as a fraction of maximal prothrombinase activity. Further details about this methodology are provided in **Appendix E1**. For the computational protocol of tracking the platelet-like particles, a cluster of approximately 1,600 identical platelet-like particles was seeded, uniformly spaced, at cross sections of venous and arterial lumens at the same distance from the tip of each modeled catheter. Each individual particle was then tracked backward and forward in its motion within the fluid domain, thereby recomposing the backward and forward segments in one trajectory. As a result, shear-induced activation state is captured for all platelets entering or moving out from the distal tip and side holes. The evolution of the system was followed for a simulated time sufficient for all platelet-like particles to leave the fluid domain.

Analysis of Recirculation

Recirculation of dialyzed blood was evaluated by computationally labeling blood in the venous lumen of each catheter and solving a convection–diffusion equation to quantify the percentage of labeled blood recirculating inside the arterial lumen. This allows consideration of the transport of a well defined concentration of dialyzed blood as a problem of transport of a scalar; recirculation of dialyzed blood was then evaluated in terms of the quantity of scalar movement from the venous lumen of the catheter to the arterial lumen.

Deflection of Dialyzed Blood Away from the Venous Lumen

The average deflection angle for fluid pathlines exiting from the venous tip of each catheter was also calculated. This angle is defined as the angle that the local tangent at each pathline forms with respect to the long axis of the SVC model.

RESULTS

Impact of Tip Design on Overall Catheter Hemodynamics

The **Table** summarizes the local Reynolds numbers and proportions of flow within the distal lumens and side holes of all the catheter models. At distal catheter tips, local Reynolds numbers ranged from 104 to 515 in the arterial lumen and from 17 to 909 in the venous lumen; within side holes, the highest Reynolds number, 515, was seen in the Palindrome catheter in the arterial

Table. Reynolds Numbers and Split Flow Proportions through Distal Tip and Side Holes of Each Catheter

Lumen	Reynolds Number	Split Flow Proportion (%)
Arterial		
VectorFlow		
Distal tip	496	53
Side holes	412	47
GlidePath		
Distal tip	224	24
Distal side holes	214	26
Proximal side holes	401	50
Palindrome		
Distal tip	104	14
Side holes	515	86
Venous		
VectorFlow		
Distal tip	909	84
Side holes	35	16
GlidePath		
Distal tip	720	78
Distal side holes	17	2
Proximal side holes	48	20
Palindrome		
Distal tip	547	73
Side holes	249	27

For the GlidePath model, distal side holes are designated as the holes closest to the distal tip.

configuration. Results summarized in the Table demonstrate that the flow inside the catheter models at locations where intricate hemodynamics occur is laminar, and that the assumption of laminar flow for the present study is valid. Considering flow repartition among distal lumens and side holes, it can be observed in the Table that the number and size of side holes play a major role in the withdraw phase, with the VectorFlow catheter characterized by the lowest percentage of flow rate through side holes (44%), compared with the highest percentages for the GlidePath (76%) and Palindrome catheters (86%). As expected, blood moves out of the catheters predominately from the distal lumen (84% for VectorFlow catheter, 78% for GlidePath catheter, and 74% for Palindrome catheter).

Analysis of Thrombogenic Flow Patterns

A comprehensive visualization of the flow features characterizing the streaming of blood inside the arterial and venous lumens of Palindrome, GlidePath, and VectorFlow catheters is presented in Figure E1 and Videos E1–E6 (available online at *www.jvir.org*). Small reattachment/separation regions were observed downstream of the side holes. These regions were common to all catheters and were characterized by 3D fluid structures differing in terms of extension and location, as determined by the different geometric characteristics.

Flow separation regions were observed within the arterial lumen of all three catheter models as a result of the perturbation of flow from the distal tip and side holes. Figure 2 depicts the extent of flow separation regions along the arterial lumen catheter tip of Palindrome, GlidePath, and VectorFlow catheters by color-encoding the isosurfaces of blood velocity components with flow in the direction opposite to the main direction of the flow. Wide regions of flow separation downstream of the Palindrome catheter side slot and close to the distal tip were observed in forward and reversed line configurations. The GlidePath catheter was characterized by small flow separation regions located downstream of the side holes and the distal tip in forward direction of flow, but, when run in the reversed configuration, a wide flow separation region was seen at the distal tip as a result of the geometric asymmetry from its distal guide wire aperture. The VectorFlow catheter showed small regions of flow separation similar to the GlidePath catheter when the catheter was run in the forward configuration; line reversal of the VectorFlow catheter did not produce a discernible increase in flow separation (Fig 2).

The GlidePath catheter showed the highest percentage of inverted velocity within the arterial lumen (6.7% of blood volume in forward direction, 6.8% of blood volume in reversed direction), followed by the Palindrome catheter (5.6% forward, 5.6% reversed) and VectorFlow catheter (3.3% forward, 3.7% reversed). Blood pathline analysis showed that the inverted velocity blood flow in the GlidePath catheter also derives from geometric asymmetry of the distal guide wire aperture producing flow perturbation when run in reversed configuration.

Analysis of Shear-Induced Platelet Activation

To compare the shear-induced platelet activation potential of the catheters, the final PAS was calculated as the mean value of all the activation levels sustained by all platelet-like trajectories moving within the catheter lumens. Figure 3 shows mean PAS values in the arterial and venous lumens for each catheter model. Platelets leaving the venous lumen experienced higher levels of activation than those leaving the the arterial lumen. This feature is common to all the catheter

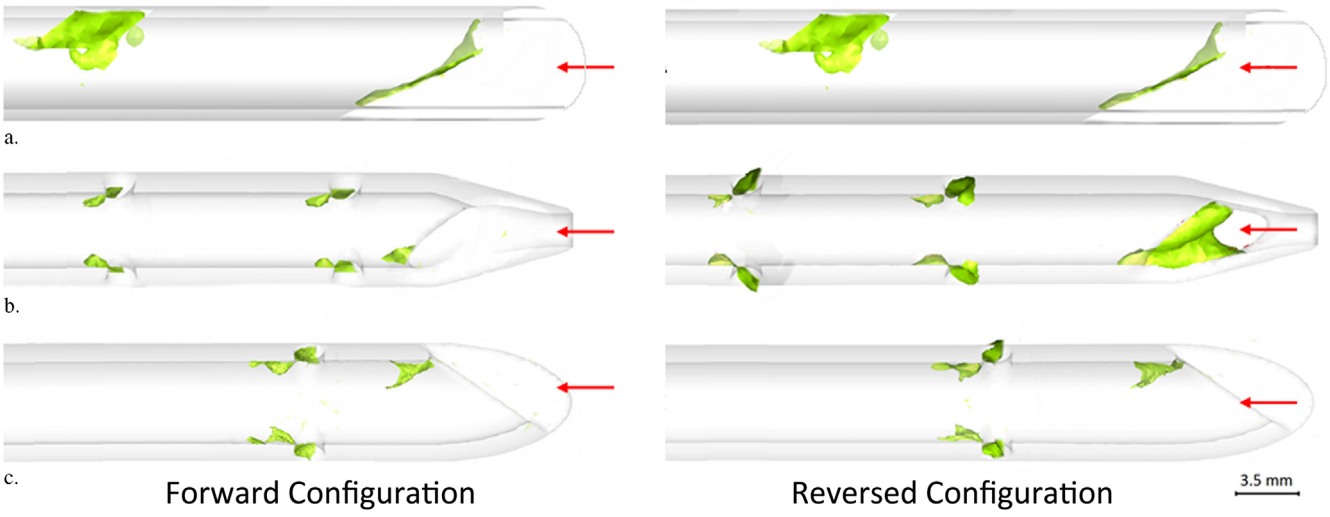

Figure 2. Flow separation regions for Palindrome **(a)**, GlidePath **(b)**, and VectorFlow **(c)** catheters in forward and reversed directions within the arterial lumen. The scale at the bottom of the image allows for quantitative analysis of the spatial extension of regions of disturbed flow inside the lumen; areas of flow separation appear in green. Red arrows indicate the main direction of flow.

models, and it can be ascribed mainly to the high-velocity jet-like structures characterizing the outflow of the catheter ports. Marked differences in the mean PAS of the venous lumens were observed, with the Palindrome catheter exhibiting venous lumen mean PAS levels (1.23×10^{-5}) that were 345% and 255% higher than the VectorFlow catheter (2.77×10^{-6}) and the GlidePath catheter (3.46×10^{-6}), respectively.

Within the arterial lumen, smaller differences among Palindrome, GlidePath, and VectorFlow catheters were observed (ie, 1.32×10^{-6} for Palindrome, 1.69×10^{-6} for GlidePath, and 2.49×10^{-6} for VectorFlow). The highest difference was observed between mean arterial lumen PAS values of the Palindrome and VectorFlow catheters (47%). Arterial and venous PAS values were averaged to assess the overall platelet activation potency of each catheter (dashed lines in Fig 3). As a result, the lowest overall PAS values were exhibited by the GlidePath (2.63×10^{-6}) and VectorFlow catheters (2.63×10^{-6}), whereas the Palindrome catheter exhibited an overall platelet activation potency (6.81×10^{-6}) that was 159% higher than the other catheter models.

Analysis of Recirculation

A negligible ($< 0.5\%$) level of recirculation was found to affect all the catheter models. Relative to the other catheter designs, the VectorFlow catheter recirculation potential was found to be the highest, albeit well below clinically relevant values. Similar values of recirculation were found in all three catheter models when run in reversed configuration (Fig 4).

To further characterize the phenomenon of recirculation of dialyzed blood related to the design features of the devices, the mean deflection angle of pathlines moving out from the venous lumen was calculated at a distance of one to five SVC diameters from the catheter tip. The results are depicted in Figure 5. By comparing deflection angles of pathlines in the different models, it is seen that the Palindrome model produces an approximately

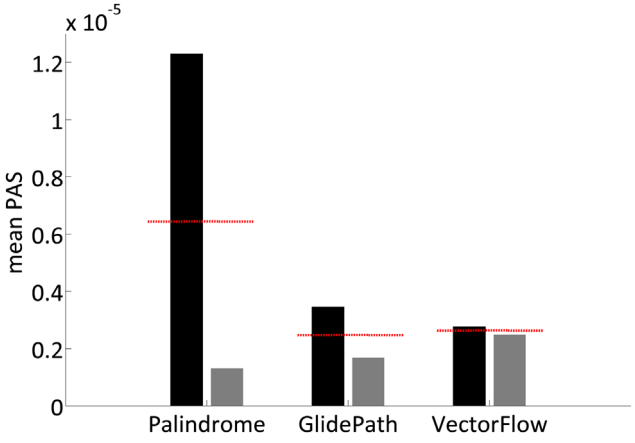

Figure 3. Mean PAS values for venous (black) and arterial (grey) lumens. Dashed line represents the mean of arterial and venous PAS values.

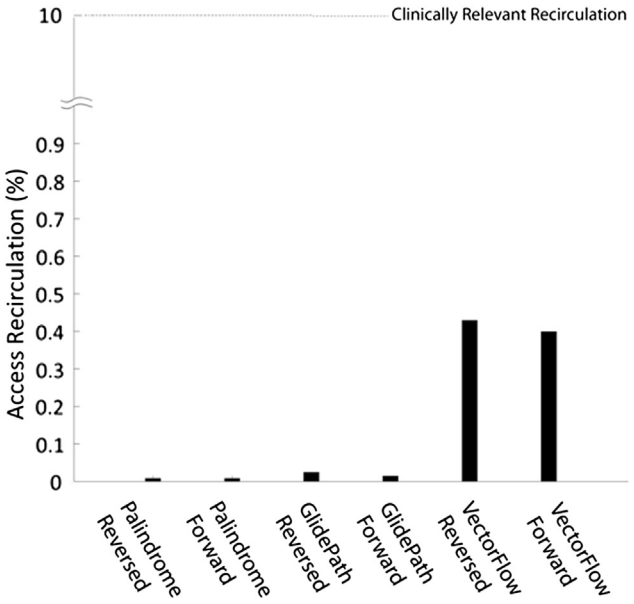

Figure 4. Recirculation of the Palindrome, GlidePath, and VectorFlow catheters in reversed and forward direction as a percentage of access recirculation. The dashed line denotes clinically significant recirculation as defined by the Kidney Disease Dialysis Outcomes Quality Initiative (2).

straight jet-like structure moving out of the venous lumen (negative mean angle deflection between -0.2° and -0.94°), whereas the GlidePath catheter design features, consisting of helically-shaped transition zones in its distal lumens, deflect the streaming blood with larger angles (as high as -9°). The blood streaming out of the VectorFlow catheter is characterized by the presence of a markedly helical flow structure (Fig 5) with a maximal deflection angle of -14°, attributed to the helically-shaped transition zones of the catheter. This feature of the flow field is also confirmed by the switch from negative to positive deflection angles when venous outflow reaches two diameters of distance from the catheter tip.

From these findings, the low recirculation in the VectorFlow catheter can be attributed to a balancing effect of flow deflection from the design of its distal tip and the increased recirculation generated as a consequence of size, position, and dimensions of side holes.

DISCUSSION

Chronic dialysis catheters remain widely used as a bridge therapy for patients awaiting permanent access placement or maturation, and when remaining options for permanent access have been depleted. In 2011, more than 27% of patients undergoing dialysis on a prevalent basis in the United States had catheters, and approximately 80% of patients who began hemodialysis in the United States did so through a catheter (1). Despite widespread use, catheters are the least desirable form of access in view of higher rates of infection and dysfunction compared with grafts and fistulae (2).

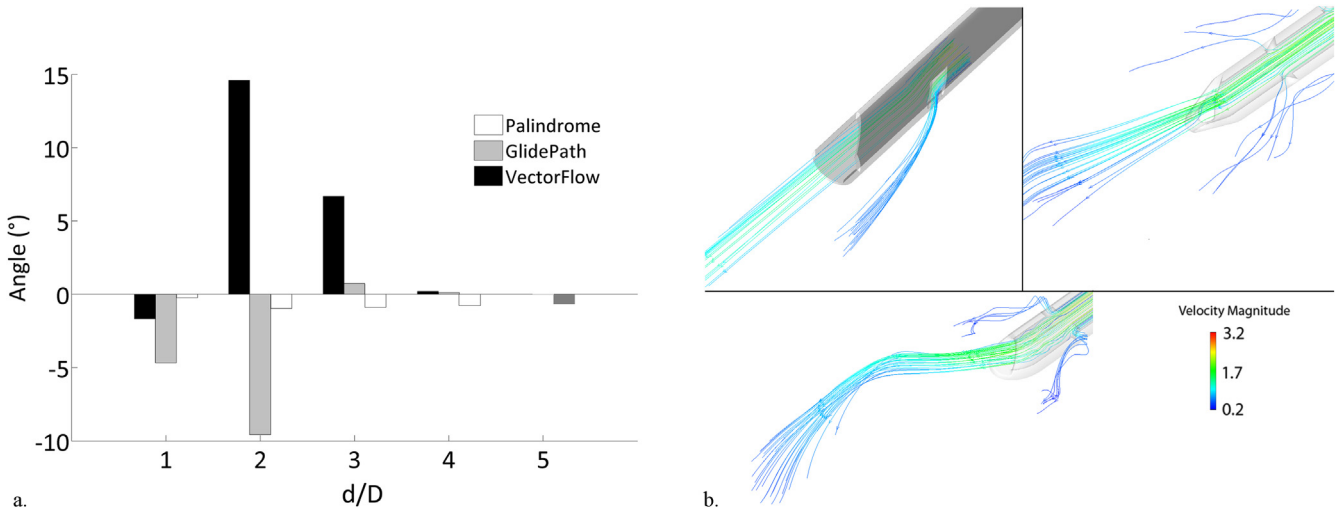

Figure 5. **(a)** Mean angle deflection of flow pathlines at a distance of one to five SVC diameters downstream of the distal tip of the catheter in forward configuration. **(b)** Representation of blood streamlines exiting venous lumen in Palindrome, GlidePath, and VectorFlow catheters colored by velocity magnitude (in meters per second).

Until viable alternatives to catheters can be found, catheter performance needs to improve and catheter-related morbidity needs to decrease. Various strategies have been used, including antithrombotic (14) and/or antimicrobial (15) surface coatings, antimicrobial lock solutions (16), and catheter tip modifications intended to improve flow characteristics and decrease recirculation (17).

Early hemodialysis catheter tip designs from the 1980s were step-tip configurations, as typified by the Quinton–Mahurkar catheter (Covidien, Dublin, Ireland). These catheters functioned well in the short term but required precise tip positioning to enable adequate flow (18). Reversing line configurations in step-tip catheter designs produced recirculation levels exceeding 25%, attributed to the close proximity of the arterial and venous lumens, and vein wall apposition to the arterial lumen (19). A strategy of spatially separating venous and arterial lumens was employed by the Tesio catheter introduced in 1994, whereby the arterial and venous lumens were free-floating and completely independent of each other. In 1996, the Ash Split Cath was developed, in which the arterial and venous lumens remained separate for a substantial portion of their tips but within a single device. The Tesio and Ash Split Cath designs (Medcomp, Harleysville, Pennsylvania) were less susceptible to positioning problems, and recirculation was reduced given the physical separation between the arterial and venous lumens (5,20,21). In 2005, the Palindrome symmetrical-tip catheter was introduced, which enabled aspiration and return of dialyzed blood through lumens that terminated at the same position within the device. By offsetting the lumens 180° and separating them through a septum with angled cross-cuts, the Palindrome catheter produced minimal admixture of arterial and venous blood, with low recirculation even when arterial and venous lines were reversed (22). A recent randomized trial comparing the Palindrome catheter versus a step-tip design (23) found a significantly higher dysfunction-free catheter patency rate at 60 days favoring the Palindrome device (78.9% vs 54.4%).

Two additional symmetrical-tip catheters have recently been introduced in the United States: the GlidePath catheter in 2013 and the VectorFlow catheter in 2014. The GlidePath catheter has curved distal apertures on opposing sides of the catheter, which are angled to minimize admixture of blood. The VectorFlow catheter has helically contoured arterial and venous apertures to produce a spiral, 3D transition of blood entering and leaving the catheter; these vectors are opposed to minimize admixture of dialyzed and nondialyzed blood.

We are aware of no clinical trials that have been performed to compare the performance of these three symmetrical-tip catheters, so a comparison of these devices based on CFD was sought to evaluate whether differences exist that could have clinical implications for the performance of these devices. Computational modeling is increasingly used in the development and assessment of medical devices, as it is able to simulate many complex physiologic conditions to generate data of medical device performance that would otherwise take months or years with the use of bench and preclinical in vivo models.

Flow within the shaft of a dual-lumen dialysis catheter is laminar, notwithstanding complex flow structures that may occur near the distal tip or side holes of a catheter. An important phenomenon in these devices is that of flow separation, whereby coherent patterns of laminar flow become disrupted by blood flowing in a direction opposite to the main direction of flow, forming a low-velocity recirculation eddy. The resultant slowing and stagnation of the bloodstream can promote thrombus formation and development (24). The Palindrome catheter was found to have the largest regions of flow separation, with these regions most prominent around the distal tip and the side slots of the catheter. The GlidePath and VectorFlow

catheters had areas of flow separation that were similar to each other, although greater in number for the GlidePath device because of its two additional side holes (which are flow separation generators). As seen in **Figure 2**, flow stagnation regions were found most prominently around catheter side holes and terminal apertures where laminar flow entering from the catheter tip becomes interrupted by side-hole inflow with resultant areas of flow reversal (ie, competitive flows). The hole at the venous lumen tip of the GlidePath device (used for guide wire insertion of the device) was also a prominent source of flow separation, in that line reversal of this device produced a marked increase in flow separation when this lumen was reversed in the arterial direction.

The tendency of each device to cause shear-induced platelet activation and aggregation during typical flow conditions of dialysis was also compared by using a previously validated computational model (8,9). Historically, the development of blood recirculating devices has focused on hemolysis as an indicator of flow-induced blood trauma (25). More recent work (26) has shown that device thrombogenicity is largely driven by platelet activation. Red blood cells are relatively resistant to mechanical effects of shear forces compared with platelets; platelets are more rigid and experience shear-induced activation at an order of magnitude less than what is required for hemolysis of red blood cells (26). We observed the highest potential for shear-induced platelet activation within the Palindrome catheter, with similarly lower levels within the GlidePath and VectorFlow catheters.

Catheter recirculation decreases the efficiency of solute clearance, and can result in the need for longer dialysis. Recirculation was very low with each catheter studied, with levels less than 1/20th of the National Kidney Foundation Kidney Disease Dialysis Outcomes Quality Initiative threshold of 10% of clinically significant recirculation (27), and concordant with what has been reported with symmetric-tip catheters in animal and clinical studies (6,23).

A previously studied design of the VectorFlow catheter without side holes found the catheter had no detectable recirculation in CFD in bench and animal models of hemodialysis (9). The lack of recirculation was attributed to the flow deflection that occurs from the helical transition zone at the distal tip of the device, whereby dialyzed blood is deflected away from the catheter in a vector 180° away from blood entering the catheter. However, that design of the VectorFlow did not include side holes.

In the present study, the flow deflection properties of each catheter were compared. The VectorFlow catheter (with side holes) continues to produce a deflection of blood away from the catheter. This phenomenon is not seen with the Palindrome catheter, as it does not have a flow-deflecting interface at the tip of the catheter to alter the vector of dialyzed blood leaving the catheter. The GlidePath catheter, which like the VectorFlow also has helically-shaped transition zones at its distal tip, did produce a component of flow deflection at its tip as a result of the curvature of the distal lumens, which change the direction of blood exiting the distal tip of the catheter (**Fig 5**).

The present study has several limitations. Catheters were compared at a single flow rate value (400 mL/min), and differing performance may have been observed at varying flow rates. Current clinical practice is to place the tip of chronic dialysis catheters within the right atrium, whereas an SVC model was used to provide uniform conditions for catheter assessment and performance comparison. There is as yet no robust CFD model of the right atrium as a result of wide variation in patient anatomy, effects of inflow from the inferior vena cava, and variation in blood flow and direction from the tricuspid valve. Notwithstanding the robustness of CFD modeling, clinical performance of these vascular devices can be definitively compared only through well designed, randomized prospective trials. Other possible limitations could arise from assuming blood as a Newtonian fluid, as it is well known that blood is a non-Newtonian fluid with a shear thinning behavior. However, previous findings (10) observed that shear rate values throughout the regions of interest inside hemodialysis catheters are high enough to neglect the non-Newtonian blood behavior (8). Moreover, the Newtonian fluid hypothesis does not compromise the generality of the conclusions.

In conclusion, substantial differences in catheter performance were observed in terms of CFD. The Palindrome catheter exhibited larger areas of flow stagnation as a result of flow separation/reattachment from the combined effects of its distal tip and larger side slots. It also showed the highest mean level of shear-induced platelet activation potency. Both attributes are considered risk factors for catheter thrombosis in clinical use. All three catheters exhibited minimal recirculation; the low recirculation seen with the Palindrome and GlidePath devices is mostly attributable to the presence of a wide septum dividing arterial and venous lumens. Conversely, the low recirculation seen with the VectorFlow device was attributable to flow deflection from the design of its distal tip (even in the presence of a smaller interposed septum between lumens); this feature partially cancels out the recirculation generated as a result of size, position, and dimension of the VectorFlow side holes). These findings suggest that catheter tip design remains an important functional attribute of symmetric chronic dialysis catheters, and further investigation is warranted in randomized clinical trials.

REFERENCES

1. U.S. Renal Data System, USRDS 2013 Annual Data Report: Atlas of Chronic Kidney Disease and End-Stage Renal Disease in the United States (Table D7). Bethesda, MD: National Institutes of Health, National Institute of Diabetes and Digestive and Kidney Diseases, 2014.
2. Dhingra RK, Young EW, Hulbert-Shearon TE, Leavey SF, Friedrich KP. Type of vascular access and mortality in U.S. hemodialysis patients. Kidney Int. 2001; 60:1443–1451.

3. Tan J, Mohan S, Herbert L, Anderson H, Cheng JT. Identifying hemodialysis catheter recirculation using effective ionic dialysance. ASAIO Journal 2012; 58:522–525.
4. Sehgal AR, Dor A, Tsai AC. Morbidity and cost implications of inadequate hemodialysis. Am J Kid Dis 2001; 37:1223–1231.
5. Trerotola SO, Kraus M, Shah H, Namyslowski J, Johnson MS, Stecker MS, Ahmad I, McLennan G, Patel NH, O'Brien E, Lane KA, Ambrosius WT. Randomized comparison of split tip versus step tip high-flow hemodialysis catheters. Kidney Int. 2002; 62:282–289.
6. Kakkos SK, Haddad GK, Haddad RK, Scully MM. Effectiveness of a new tunneled catheter in preventing catheter malfunction: a comparative study. J Vasc Interv Radiol 2008; 19:1018–1026.
7. Grigioni M, Daniele C, Morbiducci U, Di Benedetto G, D'Avenio G, Del Gaudio C, Barbaro V. Computational model of the fluid dynamics of a cannula inserted in a vessel: incidence of the presence of side holes in blood flow. J Biomech 2002; 35:1599–1612.
8. Mareels G, De Wachter DS, Verdonck PR. Computational fluid dynamics analysis of the Niagara hemodialysis catheter in a right heart model. Artif Organs 2004; 28:639–648.
9. Clark TWI, Van Canneyt K, Verdonck P. Computational flow dynamics and preclinical assessment of a novel hemodialysis catheter. Semin Dial 2012; 25:574–578.
10. Mareels G, Kaminsky R, Eloot S, Verdonck PR. Particle image velocimetry-validated, computational fluid dynamics–based design to reduce shear stress and residence time in central venous hemodialysis catheters. ASAIO Journal 2007; 53:438–446.
11. Morbiducci U, Ponzini R, Nobili M, Massai D, Montevecchi FM, Bluestein D, Redaelli A. Blood damage safety of prosthetic heart valves. Shear induced platelet activation and local flow dynamics: a fluid-structure interaction approach. J Biomech 2009; 42:1952–1960.
12. Grigioni M, Morbiducci U, D'Avenio G, Di Benedetto G, Del Gaudio C. A novel formulation for blood trauma prediction by a modified power law mathematical model. Biomech Mod Mechanobiol 2005; 4(4):249–260.
13. Nobili M, Sheriff JE, Morbiducci U, Redaelli A, Jesty J, Bluestein D. Platelet activation due to hemodynamic shear stresses: damage accumulation model and comparison to in vitro measurements. ASAIO J 2008; 54:64–72.
14. Clark TWI, Jacobs D, Charles HW, Kovacs S, Aquino T, Erinjeri J, Benstein JA. Comparison of heparin coated and conventional split-tip hemodialysis catheters. Cardiovasc Intervent Radiol 2009; 32:703–706.
15. Trerotola SO, Johnson MS, Shah H, Namyslowski J, Johnson MS, Stecker MS, Ahmad I, McLennan G, Patel NH, O'Brien E, Lane KA, Ambrosius WT. Tunneled hemodialysis catheters: use of a silver-coated catheter for prevention of infection—a randomized study. Radiology 1998; 207:491–496.
16. Moore CL, Besarab A, Ajluni M, Soi V, Peterson EL, Johnson LE, Zervos MJ, Adams E, Yee J. Comparative effectiveness of two catheter locking solutions to reduce catheter-related bloodstream infection in hemodialysis patients. Clin J Am Soc Nephrol 2014; 9:1232–1239.
17. Ash SH. Advances in tunneled central venous catheters for dialysis: design and performance. Semin Dial 2008; 21:504–515.
18. Schwab SJ, Buller GL, McCann RL, Bollinger RR, Stickel DL. Prospective evaluation of a Dacron cuffed hemodialysis catheter for prolonged use. Am J Kidney Dis 1988; 11:166–169.
19. Twardowski ZJ, Van Stone JC, Haynie JD. All currently used measurements of recirculation in blood access by chemical methods are flawed due to intradialytic disequilibrium or recirculation at low flow. Am J Kidney Dis 1998; 32:1046–1058.
20. Perini S, LaBerge JM, Pearl JM, et al. Tesio catheter: radiographically guided placement, mechanical performance, and adequacy of delivered dialysis. Radiology 2000; 215:129–137.
21. Ash SR, Mankus RA, Sutton JM. Survival and hydraulic function of the Ash Split Cath hemodialysis catheter. Nephrologie 2001; 22:403–405.
22. Tal MG. Comparison of recirculation percentage of the Palindrome catheter and standard hemodialysis catheters in a swine model. J Vasc Interv Radiol 2005; 16:1237–1240.
23. Hwang HS, Kang SH, Choi SR, Sun IO, Park HS, Kim Y. Comparison of the Palindrome vs step-tip tunneled hemodialysis catheter: a prospective randomized trial. Semin Dial 2012; 25:587–591.
24. Bluestein D, Chandran KB, Manning KB. Towards non-thrombogenic performance of blood recirculating devices. Ann Biomed Eng. 2010; 38 (3):1236–1256.
25. Paul R, Marseille O, Hintze E, Huber L, Schima H, Reul H, Rau G. In vitro thrombogenicity testing of artificial organs. Int. J. Artif. Organs 1998; 21(9):548–552.
26. Klaus S, Korfer S, Mottaghy K, Reul H, Glasmacher B. In vitro blood damage by high shear flow: human versus porcine blood. Int. J. Artif. Organs 2002; 25:306–312.
27. National Kidney Foundation. Clinical practice guidelines for vascular access. Am J Kidney Dis 2006; 48(Suppl 1):S176–273.

INVITED COMMENTARY

Numerical/Experimental Synergy: More Than Just a Reality Check

Peter D. Ballyk, MD, PhD

ABBREVIATIONS

CFD = computational fluid dynamics, SVC = superior vena cava

From the Department of Diagnostic Imaging, St. Joseph's Health Centre, University of Toronto, 30 The Queensway, Toronto, ON, Canada M6R 1B5. Final revision received and accepted December 5, 2014. **Address correspondence to** P.D.B.; E-mail: peterballyk@gmail.com

The author has not identified a conflict of interest.

J Vasc Interv Radiol 2015; 26:259–261

http://dx.doi.org/10.1016/j.jvir.2014.12.003

In "Comparison of Symmetrical Hemodialysis Catheters Using Computational Fluid Dynamics" (1), Clark and coworkers use computational fluid dynamics (CFD) to analyze the hemodynamics of three symmetrical permanent hemodialysis catheters. Based on previous publications, the hemodynamic characteristics that may influence catheter function are identified and described, and then CFD is used to quantify and compare these characteristics between catheters. The catheters

APPENDIX E1: COMPUTATIONAL SETTINGS APPLIED FOR CATHETER FLOW DYNAMICS SIMULATIONS

The set of conditions applied at boundaries, taking the Palindrome device as an example, is schematized in **Figure E1**. Each catheter model was coaxially placed inside a cylindrical conduit (18 mm in diameter), representing the superior vena cava. To ensure fully developed velocity profiles at the inlet and to minimize the influence of outlet boundary conditions, straight flow extensions were added to the inlet and outlet faces of the model. Technically, 200-mm-long inlet and 100-mm-long outlet flow extensions were added, reaching a total axial extent of the computational domain of 480 mm. More detailed, steady-state flow simulations were carried out imposing the following boundary conditions: (i) a constant 3-L/min flow rate was prescribed at the SVC inlet section (T1, **Fig E1**) in terms of flat velocity profile; (ii) reference pressure was set at the outlet section of the SVC (T2, **Fig E1**); (iii) a constant flow rate of 400 mL/min was prescribed at the venous inlet section of the catheter (V1, **Fig E1**) in terms of flat velocity profile; (iv) a flow rate value equal to 400 mL/min was prescribed as outflow boundary condition at the arterial lumen of the catheter (A2, **Fig E1**) in terms of constant mass flow. All walls were assumed as rigid; the no-slip condition was applied.

For the finite volume method-based discrete solution of the governing equation of motion over the numerical grid, the segregated solver with Semi-Implicit Method for Pressure-Linked Equations scheme was used. Second-order accuracy was used for pressure and second-order upwind for momentum. As for the quantification of access recirculation percentage, Quadratic Upwind Interpolation for Convective Kinetics discretization scheme was applied for the convection–diffusion scalar transport equation solved for the dialyzed labeled blood, guaranteeing optimal accuracy to the numeric problem solution. Convergence was accepted when the residuals of continuity and velocity decreased to less than 10^{-6}. Simulations have been run in an eight-workstation parallel architecture (Linux environment with a SUN cluster SunFire X4450; Oracle, Redwood City, California).

Analysis of Shear-Induced Platelet Activation

We used a method that performs a comprehensive analysis of platelet-like trajectories and their shear histories during flow through dual-lumen catheter models. The analysis uses information extracted from numeric simulations to resolve the flow field through the models of dual-lumen catheters. The extent to which these devices mechanically induce activation/damage of

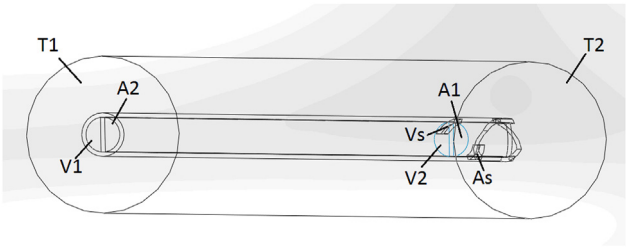

Figure E1. Conditions applied at the permeable boundaries. Schematics of the virtual bench test setup for Palindrome model (representation is not to scale). T1 and T2 are tube inlet and tube outlet, V1 and V2 are the venous inlet and outlet, and A2 and A1 are arterial inlet and outlet, respectively. Vs and As represent the venous and arterial side holes.

platelets was evaluated by using the Lagrangian-based blood damage cumulative model proposed by Grigioni et al (1). The Lagrangian-based mathematical model is based on cellular damage theory, and accounts for the cumulative load history sustained by formed elements exposed to time-dependent stress levels. Originally developed for the evaluation of red blood cell mechanical damage (11), this model has since been adapted for the assessment of platelet activation state (PAS) under dynamic loading conditions (13). PAS quantifies the more global thrombogenic aspect of platelet prothrombinase activity, ie, its contribution to thrombin generation. Developed within a hemodynamic shearing system to produce shear stress damage to human platelets, PAS values are expressed as a fraction of maximal prothrombinase activity. A mathematical model has since been validated with the human platelet assay to calculate PAS values. Specifically, the activation state of the kth platelet can be expressed as the integral sum of infinitesimal contributions:

$$\mathrm{PAS}_k = \int_{t_0}^{t} Ca\left[\int_{t_0}^{\varphi} \tau(\xi)^{b/a} d\xi + \frac{\mathrm{PAS}_k(t_0)^{1/a}}{C}\right]^{a-1} \tau(\Phi)^{b/a} d\Phi \quad \text{(Eq. E1)}$$

where $\mathrm{PAS}_k\ (t_0)$ is the value of activation of the kth platelet at the starting time of observation t_0 (ie, senescence, or previous damage history during previous passages through a vascular access device), $\tau = \tau(t)$ is the shear stress, and $a = 1.3198$, $b = 0.6256$, $C = 10^{-5}$ are the parameters of the model (14). Using this formulation, the shear history experienced by blood cells is resolved: the effects of the shear stresses previously sustained on the subsequent activation/damage (ie, senescence) is captured by Eq. (E1), and the integral sum inside the square brackets represents the mechanical load sustained by the kth platelet moving along a specific trajectory from the initial instance.

Over the whole dataset, we also calculated the mean PAS value for each time instant from the time of

injection:

$$\mathrm{PAS}_{\mathrm{mean}}(t)=\frac{1}{N_p}\sum_{k=1}^{N_p}\mathrm{PAS}_k(t) \qquad \text{(Eq. E2)}$$

where N_p is the number of platelets moving in the fluid domain.

1. Grigioni M, Morbiducci U, D'Avenio G, Di Benedetto G, Del Gaudio C. A novel formulation for blood trauma prediction by a modified power law mathematical model. Biomech Mod Mechanobiol 2005; 4(4):249-260.